REGULAR PAPER

Complex RGB spatial light modulation with a dual-layer in-plane switching liquid crystal panel

Japanese Journal of Applied Physics **62**, 122003 (2023) **REGULAR PAPER**
https://doi.org/**10.35848/1347-4065/ad0271**

Complex RGB spatial light modulation with a dual-layer in-plane switching liquid crystal panel

Seong Woo Jang[1], Sangwon Ham[1], Wonwoo Choi[2], Byeong-Kwon Ju[1], and Hwi Kim[2*]

[1]*Display and Nanosensor Laboratory, Department of Electrical Engineering, Korea University, 145, Anam-ro, Seongbuk-gu, Seoul 02841, Republic of Korea*
[2]*Department of Electronics and Information Engineering, Korea University, Sejong Campus, Sejong 30019, Republic of Korea*

*E-mail: hwikim@korea.ac.kr

Received July 16, 2023; revised October 3, 2023; accepted October 10, 2023; published online December 1, 2023

Complex RGB spatial light modulators are required to produce full-color holographic displays. In particular, complex spatial light modulation, which modulates the amplitude and phase of incident light is essential for noiseless dynamic computer-generated hologram synthesis. The feasibility of full-color holographic image generation through the dual-layer in-plane switching liquid crystal plane is theoretically validated and experimentally demonstrated.

1. Introduction

Spatial light modulators (SLMs), which modulate the amplitude and phase of light waves, are a key component for various wave optic technologies such as digital holography,[1–3] optical communications,[4] and advanced three-dimensional (3D) microscopy.[5] In particular, digital holography, which imitates the complex light field diffracted from the object to reconstruct 3D image, has been researched and advanced with the SLM technology in recent decades. High-performance color SLMs with ultra-high resolution and low optical noise are vital for the production of commercial holographic 3D displays. Genuine flat-panel SLMs are required for emerging applications such as compact holographic augmented reality glasses and holographic head-up displays. However, the practical development of SLMs to date has been limited to amplitude-only or phase-only versions, which inevitably leads to inherent optical noise.[6,7] The SLMs can be transmissive or reflective, however, the development of flat panel-type complex SLMs of either type has been highly limited in both types. A number of studies have sought to suppress the optical noise induced by amplitude-only or phase-only SLMs using bulky optical filtering systems, which is unsuitable for industrial applications that require a compact form factor. Complex light modulation involving the simultaneous and independent modulation of both the amplitude and phase of incident light waves can prevent inherent optical noises such as conjugate noise, DC noise, and speckle noise. Therefore, the development of compact flat-panel complex SLMs with no additional filtering component has been a key research focus for holographic display technology.

Liquid crystal display (LCD) is considered as a good candidate for flat panel SLM. It has been widely used as two-dimensional display device for past half-century and therefore has well-developed infrastructure, and could manipulate the amplitude and phase of the incident light by simply applying an electric field to change the arrangement of the liquid crystals. LCDs have different characteristics depending on the type, such as twisted nematic (TN) or vertical alignment (VA), and various researches on spatial light modulation have been carried out with different types of LCDs.[8–10] Some methods have been proposed to generate complex light fields with LCD-SLMs, including macropixel[8,11] and amplitude-phase dual-layer SLMs.[12] Recently, a dual-layer in-plane switching (IPS) SLM for the single-pixel complex light modulation of monochromatic optical wave fields has been presented.[13] However, even if a modulation method achieves full-color complex light modulation, multiple SLMs would be needed in practice to realize a full-color display because of the highly wavelength-dependent modulation characteristics of single SLMs, thus leading to bulky systems.[14,15] Therefore, the full-color operation of a single SLM poses a design challenge.

In this Letter, the feasibility of the full-color RGB complex light modulation using a dual-layer IPS SLM is investigated. It is shown that a single dual-layer IPS SLM with a fixed cell gap can provide the complex light modulation of red, green, and blue light waves. The goal of this study is to demonstrate the RGB complex light modulation of a single dual-layer IPS panel. Simultaneous RGB complex light modulation via a single panel is numerically derived based on dual-layer IPS LCD modulation theory, after which an RGB complex hologram is experimentally verified.

2. Theoretical analysis

Figure 1 presents a schematic diagram of a full-color transmissive-type dual-layer IPS SLM composed of double IPS liquid-crystal layers with RGB color filters. The dual-IPS layers contribute to the simultaneous modulation of RGB incident optical waves by controlling the LC tilt angles of each IPS layer. This analysis is focused on the finding of the structural parameter conditions of the single dual-layer IPS SLM for RGB complex light modulation.

A simple Jones matrix method is employed to describe the characteristics of the transmitted light.[13,16,17] The transmission characteristics of a single pixel of the dual-layer IPS SLM are described by

$$T(\phi_1, \phi_2; \theta_1, \theta_2, \Gamma) = P(\theta_2)L(\phi_2, \Gamma)L(\phi_1, \Gamma)P(\theta_1), \quad (1)$$

where the sequential multiplication of a polarizer $P(\theta_1)$, the first IPS layer $L(\phi_1, \Gamma)$, the second IPS layer $L(\phi_2, \Gamma)$, and an analyzer $P(\theta_2)$ are represented, respectively, as

$$P(\theta_2) = \begin{pmatrix} \cos\theta_2 & -\sin\theta_2 \\ \sin\theta_2 & \cos\theta_2 \end{pmatrix} \times \begin{pmatrix} 1 & 0 \\ 0 & 0 \end{pmatrix} \begin{pmatrix} \cos\theta_2 & \sin\theta_2 \\ -\sin\theta_2 & \cos\theta_2 \end{pmatrix}, \quad (2)$$

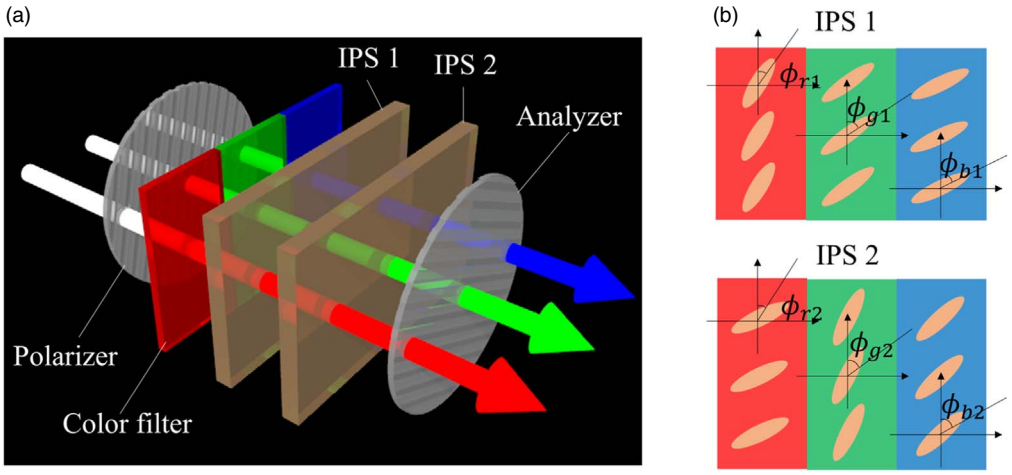

Fig. 1. (a) Schematic diagram of an RGB dual-layer IPS SLM and (b) its liquid crystal orientation.

$$L(\phi_2, \Gamma) = e^{j\frac{2\pi}{\lambda}n_o d}\begin{pmatrix}\cos\phi_2 & -\sin\phi_2\\ \sin\phi_2 & \cos\phi_2\end{pmatrix} \times \begin{pmatrix}e^{j\Gamma} & 0\\ 0 & 1\end{pmatrix}\begin{pmatrix}\cos\phi_2 & \sin\phi_2\\ -\sin\phi_2 & \cos\phi_2\end{pmatrix}, \tag{3}$$

$$L(\phi_1, \Gamma) = e^{j\frac{2\pi}{\lambda}n_o d}\begin{pmatrix}\cos\phi_1 & -\sin\phi_1\\ \sin\phi_1 & \cos\phi_1\end{pmatrix} \times \begin{pmatrix}e^{j\Gamma} & 0\\ 0 & 1\end{pmatrix}\begin{pmatrix}\cos\phi_1 & \sin\phi_1\\ -\sin\phi_1 & \cos\phi_1\end{pmatrix}, \tag{4}$$

$$P(\theta_1) = \begin{pmatrix}\cos\theta_1 & -\sin\theta_1\\ \sin\theta_1 & \cos\theta_1\end{pmatrix}\begin{pmatrix}1 & 0\\ 0 & 0\end{pmatrix}\begin{pmatrix}\cos\theta_1 & \sin\theta_1\\ -\sin\theta_1 & \cos\theta_1\end{pmatrix}, \tag{5}$$

where θ_1, θ_2, ϕ_1, ϕ_2, and d are the polarizer tilt angle, the analyzer tilt angle, the first IPS-LC tilt angle, the second IPS-LC tilt angle, and cell gap, respectively, and n_e and n_o are the extraordinary and ordinary indices of the liquid crystal, respectively. Γ is the phase retardation given by $\Gamma = 2\pi(n_e - n_o)d/\lambda$, which is wavelength-dependent. When x-directional linear polarized incident light is assumed, the output electric field could be represented as following:

$$\begin{pmatrix}E_x\\ E_y\end{pmatrix} = T(\phi_1, \phi_2; \theta_1, \theta_2, \Gamma)\begin{pmatrix}1\\ 0\end{pmatrix}. \tag{6}$$

After some manipulation of the equation, the output components E_x and E_y can then be obtained in the form of three-phase AM:

$$E_{x(y)} = E_{x(y),0} + E_{x(y),\Gamma}e^{j\Gamma} + E_{x(y),2\Gamma}e^{j2\Gamma}, \tag{7}$$

where the x-component amplitudes $E_{x,0}$, $E_{x,\Gamma}$, and $E_{x,2\Gamma}$ are given by

$$E_{x,0} = e^{j\frac{4\pi}{\lambda}n_o d}AB(A\cos\phi_2 - B\sin\phi_2) \times (C\cos\phi_1 - D\sin\phi_1)\cos\Delta\phi, \tag{8}$$

$$E_{x,\Gamma} = e^{j\frac{4\pi}{\lambda}n_o d} \times AB\begin{bmatrix}(-C\sin\phi_1 + D\cos\phi_1)(A\cos\phi_2 + B\sin\phi_2)\\ +(A\sin\phi_2 - B\cos\phi_2)(C\cos\phi_1 + D\sin\phi_1)\end{bmatrix}\sin\Delta\phi, \tag{9}$$

$$E_{x,2\Gamma} = e^{j\frac{4\pi}{\lambda}n_o d}AB(A\cos\phi_2 - B\sin\phi_2) \times (C\cos\phi_1 - D\sin\phi_1)\cos\Delta\phi, \tag{10}$$

and the y-component amplitudes $E_{y,0}$, $E_{y,\Gamma}$, and $E_{y,2\Gamma}$ are given by

$$E_{y,0} = e^{j\frac{4\pi}{\lambda}n_o d}BC(A\cos\phi_2 + B\sin\phi_2) \times (C\cos\phi_1 + D\sin\phi_1)\cos\Delta\phi, \tag{11}$$

$$E_{y,\Gamma} = e^{j\frac{4\pi}{\lambda}n_o d}BC \times \begin{pmatrix}(-C\sin\phi_1 + D\cos\phi_1)(A\cos\phi_2 + B\sin\phi_2)\\ +(A\sin\phi_2 - B\cos\phi_2)(C\cos\phi_1 + D\sin\phi_1)\end{pmatrix}\sin\Delta\phi, \tag{12}$$

$$E_{y,2\Gamma} = e^{j\frac{4\pi}{\lambda}n_o d}BC(A\cos\phi_2 - B\sin\phi_2) \times (C\cos\phi_1 - D\sin\phi_1)\cos\Delta\phi. \tag{13}$$

For the sake of convenience, the substitutions, $A = \cos\theta_2$, $B = \sin\theta_2$, $C = \cos\theta_1$, $D = \sin\theta_1$, and $\Delta\phi = \phi_2 - \phi_1$ are used. Complex light modulation can be achieved by modulating the three-phase AM form of Eq. (7). Without loss of generality, the modulation of E_x is analyzed. Parametric analysis of the modulation of E_x with respect to the structural parameters, θ_1, θ_2, and d is conducted to simultaneously maximize the complex light modulation range for RGB wavelengths. During this optimization, the wavelength dependent values of the LC refractive indices are taken into account. The extraordinary index n_e and ordinary index n_o is taken using Cauchy's equation as

$$n_e = 1.5600 + \frac{11423}{\lambda^2}, \tag{14}$$

$$n_o = 1.4694 + \frac{5549}{\lambda^2}. \tag{15}$$

The coefficients are provided by LG Display Co., which manufactured the IPS panel used in the experiments described later.

The optimal parameter condition (d^*, θ_1^*, θ_2^*) can be found by optimizing the following figure of merit:

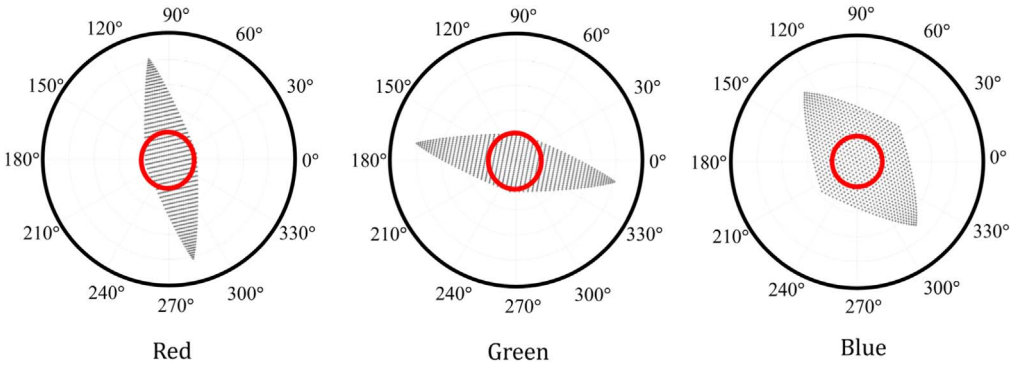

Fig. 2. Complex light modulation characteristics of the proposed dual IPS architecture for red ($\lambda_R = 633$ nm), green ($\lambda_G = 532$ nm), and blue ($\lambda_B = 473$ nm) wavelengths. The solid circles indicate the full complex light modulation range with a maximum amplitude of 0.2.

$$\left(d^*, \theta_1^*, \theta_2^*\right) = \arg\max\left(\min\left(\rho_R, \rho_G, \rho_B\right)\right), \tag{16}$$

where ρ_R, ρ_G, and ρ_B are the maximum radius of the inscribed circle in the complex light modulation range for red (633 nm), green (532 nm), and blue (473 nm) wavelengths, respectively. ρ_R can be represented as

$$\rho_R(d, \theta_1, \theta_2; \lambda_R) = \min\left(\max\left(\sqrt{E_{x,r}^2(d, \theta_1, \theta_2; \lambda_R) + E_{x,i}^2(d, \theta_1, \theta_2; \lambda_R)}\right)\right), \tag{17}$$

where $E_{x,r}$ and $E_{x,i}$ are the real and Ims of E_x, respectively. ρ_G and ρ_B are defined by the same manner for the wavelengths λ_G and λ_B. Parametric analysis of Eq. (16) finds the single condition (d^*, θ_1^*, θ_2^*) for RGB colors. The sweeping range for the polarizer angle and the analyzer angle is set from 0 to 180 degrees with 5 degree intervals, and the sweeping range for the cell gap d is set at 2.5–3.5 μm with 0.05 μm intervals, which is an allowable range for IPS-LC panel fabrication. Under each condition, the complex modulation range when the IPS-LC is tilted from minimum (0 degree) to maximum value (33.28 degree) is calculated. In each range, Eq. (17) is calculated to find the maximum value of the inscribed circle and its parametric conditions. The obtained single condition (d^*, θ_1^*, θ_2^*) results in the modulation range for RGB wavelengths presented in Fig. 2, in which the common inscribed circle ρ in the modulation space for RGB wavelengths is indicated by a solid circle. The tilt angles of the polarizer θ_1^* and the analyzer θ_2^*, and the cell gap d^* are obtained 15°, 105°, and 2.75 μm, respectively. The resulting ρ is about 0.2, which ensures full range RGB complex light modulation within a 20% amplitude range. Since the power is proportional to amplitude squared, it is interpreted that the proposed system could cover as much as 4% of the total modulation circle at the current stage. The modulation efficiency could be further increased by optimizing the design parameters, such as the maximum tilt angle of the liquid crystal.

3. Experiments

3.1. Validation of full color complex modulation

To verify the RGB complex light modulation of the designed SLM, we test the feasibility of 3D holographic image generation. A dual-layer IPS SLM is fabricated with an identical pair of 2.3 inch IPS panel precisely aligned and attached together. the display resolution of the panel is

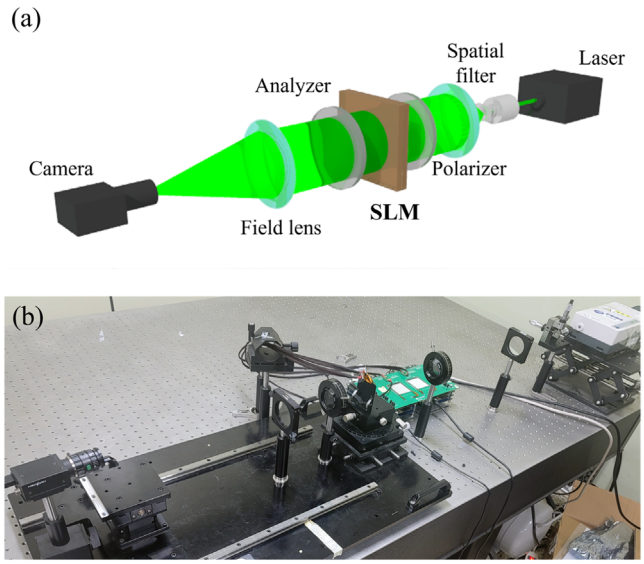

Fig. 3. (a) Schematic diagram of CGH generation and the observation system and (b) the experimental implementation.

2560 × 1600, the pixel size is 16.4 μm × 8.2 μm, the aperture ratio is 7.15%, and the thickness of the glass layer of the panel is about 100 μm, which means that the thickness of the whole device is about 400 μm. Figure 3 presents the experimental schematic and implementation. A laser beam is collimated through a spatial filter and a convex lens, then passes through the fabricated dual-layer IPS SLM. A computer generated hologram (CGH) is displayed, and its optical image is observed using a color CCD (Point Gray Grasshopper® 3) with a field lens and no additional intermediate filtering system for noise removal, which allows for a simple and compact system. The RGB lasers with wavelengths of λ_R(=633 nm) (Civilaser 3 W Semiconductor Laser), λ_G(=532 nm) (Lighthouse Photonics Sprout-G-8W), and λ_B = 473 nm (Civilaser 2500 mW Semiconductor Laser) are used in each experiment.

Initially, a far-field CGH is designed. Complex CGH $U(x, y)$ and amplitude-only CGH $A(x, y)$(=Re (U) − min (Re (U))) are designed for the word "KU" using the angular spectrum method.[14,18] For complex CGH $U(x, y)$, the LC tilt angles of each pixel of the dual-layer IPS SLM required to contribute to the complex light field are calculated using a pre-established complex light modulation table (Fig. 2), and a pair of input images for the dual-layer IPS SLM is designed based on the

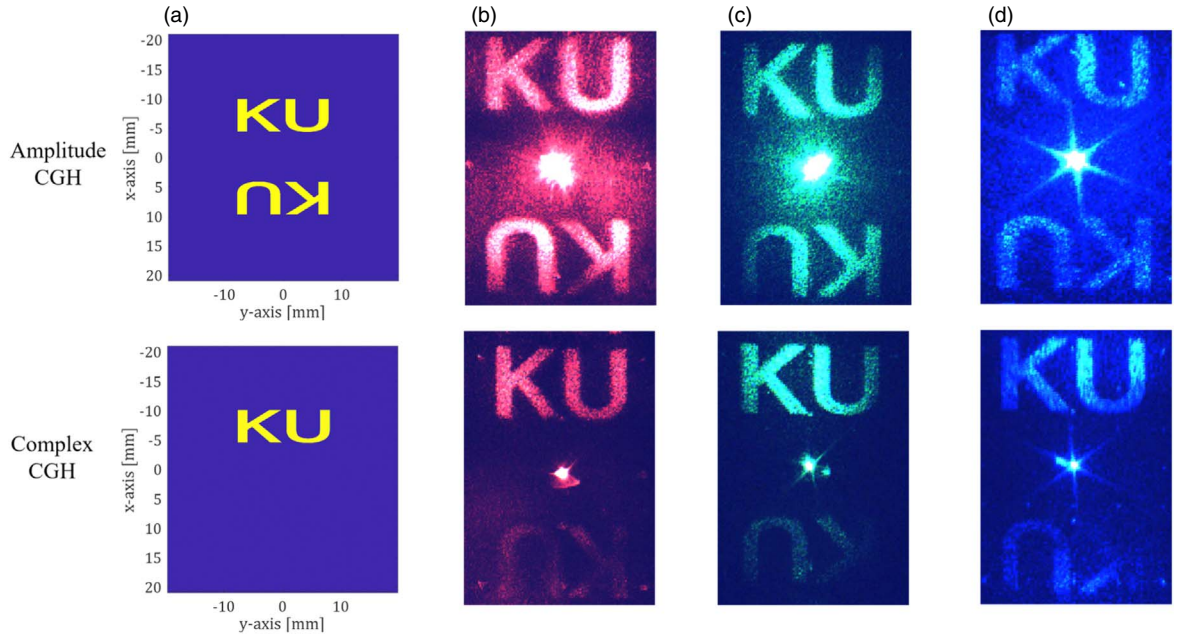

Fig. 4. Far-field CGH test with complex light modulation (left panels) and AM (right panels): (a) simulation results and (b)–(d) experimental results for red, green, and blue.

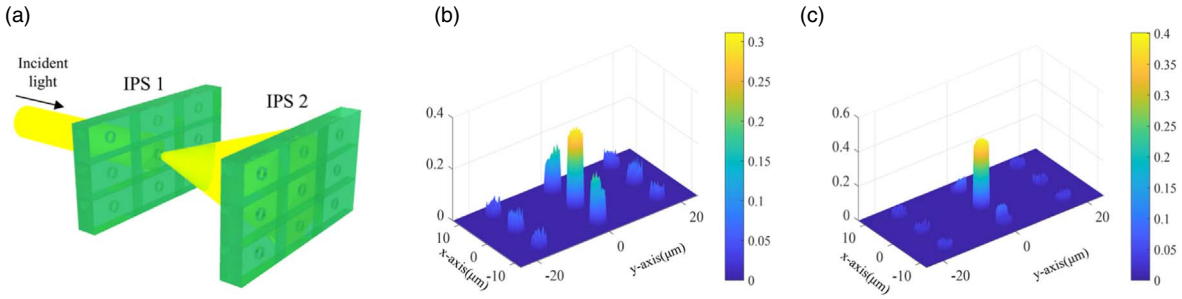

Fig. 5. Simulated crosstalk occurs at the adjacent pixels. (a) schematic figure of the simulations. (b) Result with current condition with the glass layer thickness of 100 μm. (c) Result when the glass layer thickness is reduced to 70 μm.

relationship between the LC tilt angles and the grayscale values of the input images. For the amplitude CGH $A(x, y)$ experiment, the value of $A(x, y)$ is input into a single IPS SLM.[13] Figure 4 presents the numerical simulation and experimental results of the designed far-field CGH.

The basic test investigates whether the amplitude-only CGH and the genuine complex CGH suffer from conjugate and DC noise. Figures 4(b)–4(d) show that DC and conjugate noise are drastically suppressed in the observation results for all colors using the complex CGH. Because the noise component is separated from the signal region, the signal-to-noise ratio (SNR)($=20 \log (A_{\text{signal}} / A_{\text{noise}})$) can be acquired by selecting the separated region of interest (ROI) and measuring the respective signal and noise intensity. The calculated SNR for the RGB amplitude CGH is -5.86 dB, -6.72 dB, and -5.36 dB, respectively, while that for the RGB complex CGH is significantly higher at 3.24 dB, 7.04 dB, and 2.87 dB, respectively. These results confirm that the designed dual-layer IPS system achieves complex light modulation for all RGB wavelengths.

Although the complex CGH observation results still exhibit some faint DC and conjugate noise, which reduces the SNR, this noise most likely originates from practical issues such as the crosstalk between two panels. This inter-layer crosstalk occurs as a result of diffractive spreading in the non-negligible gap between two IPS layers. The optical field passing by a pixel aperture in the first panel spreads to several pixels in the second panel. This crosstalk leads to incomplete modulation and eventually contributes to optical noise and degradation in the transmission and modulation efficiency. The inter-layer crosstalk is simulated with the angular spectrum method, based on the parameters of the fabricated dual IPS device. Figure 5 shows the simulated signal intensity of the turned-on pixel and the intensity of the crosstalk occurs at the adjacent pixels. Figure 5(b) shows the crosstalk in the current condition, and the calculated SNR is 4.86 dB, which is similar value with the observed complex CGH. Although this crosstalk does not appear to be a critical flaw for modulation at this stage, further reducing the gap between dual IPS layers would lead to better modulation performance. Figure 5(c) shows the crosstalk when the gap is reduced to 70 μm, and the SNR is improved to 15.05 dB.

3.2. Generation of 2-level complex CGH

Next, a complex CGH designed with two images located at different distances is calculated using the cascaded Fresnel transform method.[12,14,19] The target images are located at a distance of 0 cm and 20 cm, respectively, from the field lens. As with the far-field CGH, the complex light modulation

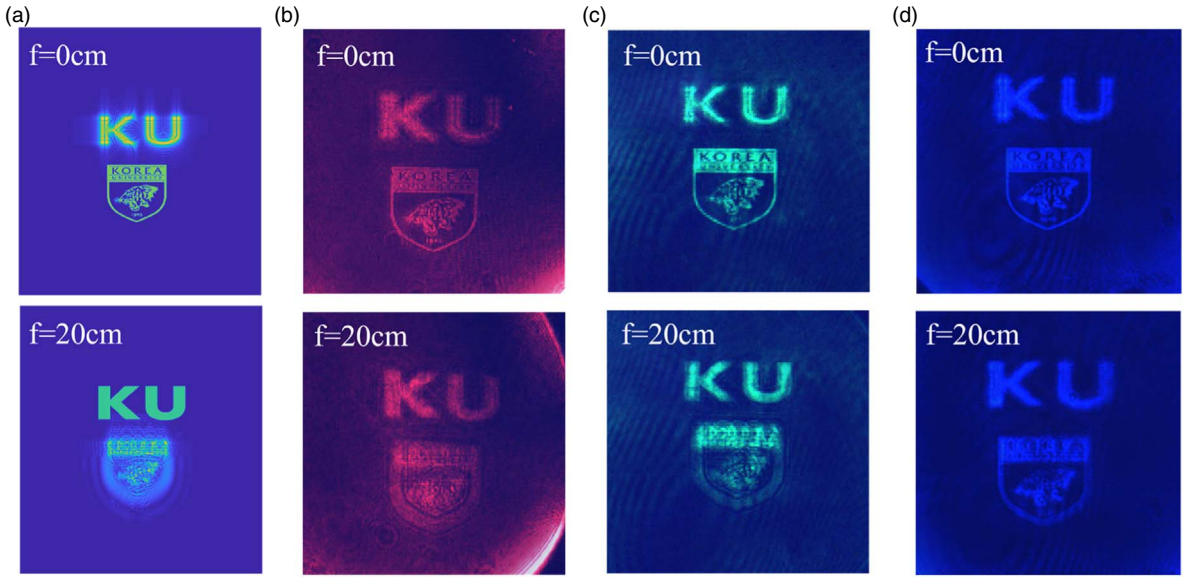

Fig. 6. Simulations and observation results of red, green and blue complex CGHs with a depth of 0 cm (upper panels) and 20 cm (lower panels).

value for each pixel in the CGH is converted to a pair of pre-calculated grayscale values to display a complex CGH on the dual-layer IPS SLM.

Figure 6(a) presents the numerical observation result for the designed CGH. An accommodation effect is observed at a focal length of 0 cm and 20 cm, where the word "KU" and the university emblem are in focus or out of focus. Figures 6(b)–6(d) show the experimental observation results for the two-depth CGH in RGB colors. In all of the results, accommodation effect is clearly observed. In other words, the image at the corresponding focal length is distinct, while the other one is blurred, and the background noise is sufficiently suppressed to allow the images to be clearly observed without an additional optical filtering system. Unfortunately, we were unable to fabricate a dual-layer IPS SLM with an RGB color filter layer, but conducted independent experiments for RGB colors using a bare dual-layer IPS SLM without color filters. Even with this limitation in our experiment, we can predict that, based on the feasibility test, a single dual-layer IPS SLM with color filters (Fig. 1) will be capable of displaying full-color CGHs.

4. Conclusions

In conclusion, we have achieved 3-phase complex light modulation with a single dual-layer IPS SLM system for all RGB wavelengths. Instead of using three SLMs for the individual RGB wavelengths, we identified a single condition to fit the modulation for the entire wavelength range, leading to a highly feasible compact holographic display device. Because genuine complex light modulation is achieved for all RGB wavelengths, full-color complex holographic display could be straightforwardly produced in a straightforward manner when a color filter is precisely aligned and attached to the dual-layer IPS SLM. However, in the present stage of development, the transmission efficiency of the system is not sufficiently high. Our next task will focus on solving this problem and enhancing the system efficiency for industrial applicability. Although simply reducing the gap between the layers would be a simple and intuitive solution to enhance the light efficiency and reduce the inter-layer optical crosstalk, further reducing the gap will not only be challenging in terms of device fabrication, but also the effect of the electrical crosstalk between two layers will become impossible to ignore. A possible solution may be placing a microlens array between the dual layers. The diffraction between the dual layers leads to loss and unwanted inter-layer crosstalk, and a micro-sized metalens array could be a good promising candidate for guiding the light diffracted from one pixel to the corresponding pixel.[20] Implementing different LC modes, such as TN or VA modes, can be also a possible solution. The point is that the total efficiency of the dual-layer system can increase if the optical efficiency of those LC modes is higher than IPS mode. It is needed to study whether the three-phase modulation equations for these modes can be found. This solution is attractive because when the LCD with better efficiency is applied, the total efficiency of the system will increase by square. Research investigating these methods is currently in progress and the resulting full-color complex CGH will be presented in our future papers.

Acknowledgments

This work was supported by Alchemist Project grant funded by Korea Evaluation Institute of Industrial Technology (KEIT) and the Korea Government (MOTIE) (Project Number: 1415179744, 20019169).

1) F. Mok, J. Diep, H. K. Liu, and D. Psaltis, "Real-time computer-generated hologram by means of liquid-crystal television spatial light-modulator," Opt. Lett. **11**, 748 (1986).
2) L. G. Neto, D. Roberge, and Y. L. Sheng, "Full-range, continuous, complex modulation by the use of two coupled-mode liquid-crystal televisions," Appl. Opt. **35**, 4567 (1996).
3) J. Hahn, H. Kim, Y. Lim, G. Park, and B. Lee, "Wide viewing angle dynamic holographic stereogram with a curved array of spatial light modulators," Opt. Express **16**, 12372 (2008).
4) S. Ahderom, M. Raisi, K. Lo, K. E. Alameh, and R. Mavaddat, "Applications of liquid crystal spatial light modulators in optical communications," Hsnmc 2002: 5th Ieee Int. Conf. on High Speed Networks and Multimedia Communications, 2002, p. 239.
5) T. H. Nguyen and G. Popescu, "Spatial light interference microscopy (SLIM) using twisted-nematic liquid-crystal modulation," Biomed. Opt. Express **4**, 1571 (2013).

6) J. P. Liu, W. Y. Hsieh, T. C. Poon, and P. Tsang, "Complex Fresnel hologram display using a single SLM," Appl. Opt. **50**, H128 (2011).
7) J. Cho, S. Kim, S. Park, B. Lee, and H. Kim, "DC-free on-axis holographic display using a phase-only spatial light modulator," Opt. Lett. **43**, 3397 (2018).
8) V. Arrizon, "Complex modulation with a twisted-nematic liquid-crystal spatial light modulator: double-pixel approach," Opt. Lett. **28**, 1359 (2003).
9) A. J. Macfaden and T. D. Wilkinson, "Characterization, design, and optimization of a two-pass twisted nematic liquid crystal spatial light modulator system for arbitrary complex modulation," J. Opt. Soc. Am. A **34**, 161 (2017).
10) I. Nys, J. Beeckman, and K. Neyts, "Fringe-field-induced out-of-plane reorientation in vertically aligned nematic spatial light modulators and its effect on light diffraction," Liq. Cryst. **48**, 1516 (2021).
11) H. Kim, C. Y. Hwang, K. S. Kim, J. Roh, W. Moon, S. Kim, B. R. Lee, S. Oh, and J. Hahn, "Anamorphic optical transformation of an amplitude spatial light modulator to a complex spatial light modulator with square pixels [Invited]," Appl. Opt. **53**, G139 (2014).
12) S. Park, J. Roh, S. Kim, J. Park, H. Kang, J. Hahn, Y. Jeon, S. Park, and H. Kim, "Characteristics of complex light modulation through an amplitude-phase double-layer spatial light modulator," Opt. Express **25**, 3469 (2017).
13) S. W. Jang, W. Choi, S. Kim, J. Lee, S. Na, S. Ham, J. Park, H. Kang, B. K. Ju, and H. Kim, "Complex spatial light modulation capability of a dual layer in-plane switching liquid crystal panel," Sci. Rep. **12**, 8277 (2022).
14) J. Roh, K. Kim, E. Moon, S. Kim, B. Yang, J. Hahn, and H. Kim, "Full-color holographic projection display system featuring an achromatic Fourier filter," Opt. Express **25**, 14774 (2017).
15) S. F. Lin and E. S. Kim, "Single SLM full-color holographic 3D display based on sampling and selective frequency-filtering methods," Opt. Express **25**, 11389 (2017).
16) J. Park, H. Yu, J. H. Park, and Y. Park, "LCD panel characterization by measuring full Jones matrix of individual pixels using polarization-sensitive digital holographic microscopy," Opt. Express **22**, 24304 (2014).
17) H. J. Cho, D. H. Kim, and Y. H. Lee, "A simple distribution model of the twist angle in an in-plane switching liquid crystal display," J. Opt. A: Pure Appl. Opt. **11**, 105409 (2009).
18) F. Shen and A. Wang, "Fast-Fourier-transform based numerical integration method for the Rayleigh-Sommerfeld diffraction formula," Appl. Opt. **45**, 1102 (2006).
19) S. Park, J. Lee, S. Lim, M. Kim, S. Ahn, S. Hwang, S. Jeon, J. Jeong, J. Hahn, and H. Kim, "Wide-viewing full-color depthmap computer-generated holograms," Opt. Express **29**, 26793 (2021).
20) S. Uenoyama and R. Ota, "40 × 40 metalens array for improved silicon photomultiplier performance," ACS Photonics **8**, 1548 (2021).